Stimulus-Dependent Interaction between the Visual Areas 17 and 18 of the 2 Hemispheres of the Ferret (*Mustela putorius*)

Valeri A. Makarov[1], Kerstin E. Schmidt[2], Nazareth P. Castellanos[1], Laura Lopez-Aguado[1] and Giorgio M. Innocenti[3]

[1]Department of Applied Mathematics, School of Optics, Universidad Complutense de Madrid, 28037 Madrid, Spain, [2]Max Planck Institute for Brain Research, 60528 Frankfurt, Germany and [3]Department of Neuroscience, Karolinska Institutet, S17177 Stockholm, Sweden

Valeri A. Makarov and Kerstin E. Schmidt contributed equally to this work.

To study how the visual areas of the 2 hemispheres interact in processing visual stimuli we have recorded local field potentials in the callosally connected parts of areas 17 and 18 of the ferret during the presentation of 3 kinds of stimuli: 2.5° squares flashed for 50 ms randomly in the visual field (S1), 4 full-field gratings differing in orientation by 45° and identical in the 2 hemifields (S2) and gratings as above but whose orientation and/or direction of motion differed by 90° in the 2 hemifields (S3). The gratings remained stationary for 0.5 s and then moved in 1 of the 2 directions perpendicular to their orientation for 3 s. We compared the responses in baseline conditions with those obtained whereas the contralateral visual areas were inactivated by cooling. Cooling did not affect the responses to S1 but it modified those to S2 and to S3 generally increasing early components of the response while decreasing later components. These findings indicate that interhemispheric processing is restricted to visual stimuli which achieve spatial summation and that it involves complex inhibitory and facilitatory effects, possibly carried out by interhemispheric pathways of different conduction velocity.

Keywords: cooling, corpus callosum, ferret, interhemispheric interactions, visual cortex

Introduction

In the visual system, the representation of the retina is divided between the 2 hemispheres along a line corresponding to the naso-temporal decussation of ganglion cell axons at the chiasm. This line is un-sharp and, therefore, a narrow strip of the visual field midline is represented in both hemispheres. A nagging question (e.g., Hubel and Wiesel 1967; Berlucchi 1972; Payne et al. 1991; Ptito 2003) is whether this bilateral representation of the retina is sufficient to re-establish the functional continuity between the 2 hemi-representations of the visual field or, if instead, direct connections between the visual areas of the 2 hemispheres are required. The latter is strongly suggested by the anatomical organization of callosal connections. In all species, including the ferret, which was used in this study, and in areas, which contain retinotopic maps, callosal connections are mainly or exclusively found near the representations of the midline of the visual field (Berlucchi et al. 1967; Hubel and Wiesel 1967; Shatz 1977; Innocenti 1980; Lepore and Guillemot 1982; Innocenti 1986; Manger et al. 2002).

The attempts to directly test the contribution of callosal connections to visual functions near the visual midline have provided incomplete answers. A confirmed finding was that in split-chiasm cats callosal input contributes, along the visual midline, receptive field moieties, in register with those generated through the ipsilateral, temporal retino-geniculo-cortical projection (Berlucchi and Rizzolatti 1968; Lepore and Guillemot 1982; Antonini et al. 1983; Guillemot et al. 1993; Milleret et al. 1994; Milleret and Houzel 2001; Ptito 2003). Cooling the visual areas of one hemisphere was found to either enhance or depress the responses to moving light bars in the other hemisphere, although no complete disappearance of the responses was reported (Payne et al. 1991). This suggests that in the intact animal the visual responses in 1 hemisphere are dominated by the retino-geniculo-cortical input, with the callosal afferents playing a modulatory role. Indeed, an important function of callosal connections is that of time-locking neuronal assemblies generated in the 2 hemispheres by visual stimuli such as moving bars or gratings (Engel et al. 1991; Munk et al. 1995; Kiper et al. 1999; Knyazeva et al. 1999, 2006; Carmeli et al. 2005).

To determine if the visual midline shows properties which could be ascribed to callosal connections Nakamura et al. (Forthcoming) studied the cortical responses evoked by small (1.5°) stationary stimuli of short duration (about 50 ms) using a combination of fast optical imaging, voltage sensitive dyes, and local field potentials (LFPs). Responses along the visual midline had lower amplitudes and longer latencies than in more peripheral parts of the visual field. However, these features could be ascribed to properties of the retino-geniculo-cortical input near the retinal midline, unaffected by the callosal input.

Contrary to expectation, therefore, callosal connections appeared to play no role at the midline of the visual field. The study had limitations because only discrete, short-lasting stimuli were used and the contribution of the other hemisphere to the responses was not directly assessed.

Therefore, we now reinvestigate the role of hemispheric interactions along the visual field midline by studying the consequences of inactivating the contralateral visual areas (as in Payne et al. 1991). To compare the results with those of previous studies we use small flashing squares (as in Nakamura et al. Forthcoming) but also gratings of identical or different orientations in the 2 hemifields (as in Kiper et al. 1999; Carmeli et al. 2005; Knyazeva et al. 2006). Our results suggest that the callosal connections integrate the visual field in a stimulus-specific manner. This is consistent with previous work in callosal-split patients and might provide a general framework for understanding the contribution of callosal connections in re-establishing the continuity between the hemispherically split sensory representations.

Materials and Methods

Nine female ferrets bought from a Swedish authorized breeder were prepared for the experiment and maintained under anesthesia

according to protocols conforming to Swedish and European Community guidelines for the care and use of animals in scientific experiments and approved by the ethic committee of Stockholm District.

Stimuli

During the experiment the following 3 classes of stimuli have been presented (Fig. 1A) as a rule to the same animal. S1 stimulus was a bright 2.5° square flashed for 50 ms with 0.5-s interstimulus intervals at 10 × 10 random positions covering 25° in the central portion of the visual field. We repeated the stimulus sequence 10 times at 2-s intervals.
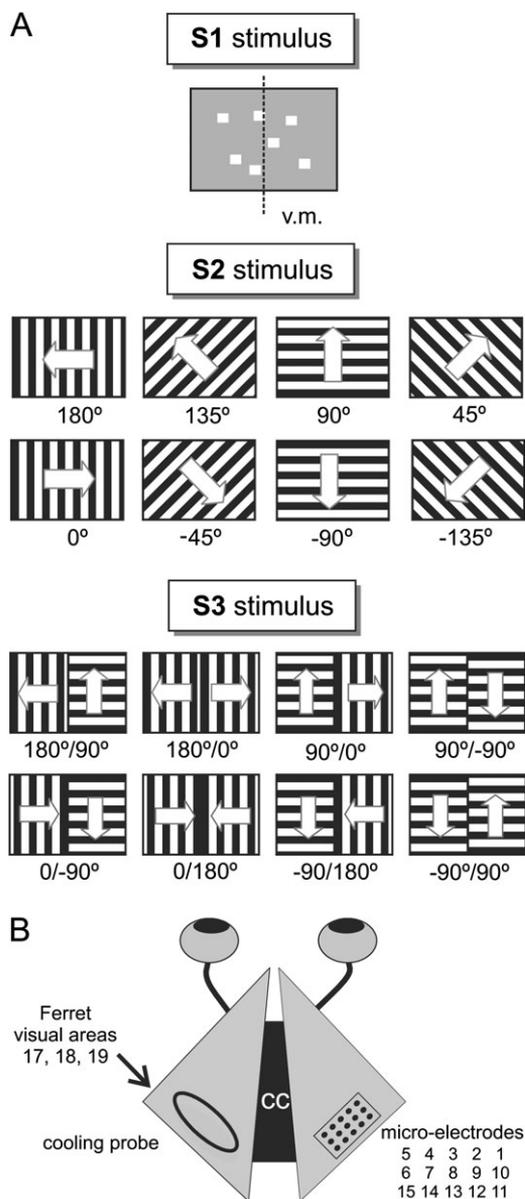

Figure 1. Experimental setup. (A) Visual stimuli used. S1 was a bright 2.5° square flashed for 50 ms at 10 × 10 random positions covering 25° in the central portion of the visual field. S2 were 30 × 40° whole-field gratings of 4 different orientations moving into the 2 orthogonal directions, centered on the midline of the visual field. S3 were gratings with either different orientations or different directions of motions in the 2 visual hemifields. The midline of the visual field (v.m.) is shown only for S1. (B) An array of 15 microelectrodes was lowered into occipital cortex of the right hemisphere of the ferret. A 3-mm × 6-mm metal cooling loop was positioned on the corresponding position of the contralateral hemisphere. Electrodes 1 and 9 were permanently disabled. The electrodes cover a 1640 × 820-μm rectangle and are spaced in 410-μm intervals.

S2 stimuli consisted of 4 full-field gratings oriented around the clock in 45° steps and identical in the 2 hemifields. S3 stimuli were gratings as above but whose orientation and/or direction of motion differed in the 2 hemifields. The stimuli remained stationary for 0.5 s and then moved in 1 of the 2 directions perpendicular to their orientation for 3 s followed by 3 s of exposure to an equiluminant gray screen. The gratings had a spatial frequency of 0.1 cycle/deg and moved at 14 deg/s.

Recordings

For recordings of LFPs, anesthesia was maintained by artificial ventilation with a mixture of N_2O (65%), O_2 (35%), and isoflurane (0.8-1.2%) supplemented with intravenous application of a muscle relaxant (pancuronium bromide, 0.25 mg/kg/h) to prevent eye movements. Pupils were dilated with atropine and neosynephrine and fitted with contact lenses. A craniotomy was made over the occipital pole of each hemisphere. LFPs were recorded from the right hemisphere using a 3 × 5 matrix of 15 tungsten microelectrodes spaced at 410 μm from each other (FHC, Bowdoinham, ME) and aimed at the border between areas 17 and 18 (Fig. 1B). The position of the microelectrodes was confirmed histologically after the experiment and they were found to record from the supragranular layers. Hand mapped receptive fields, confirmed in most cases by computerized mapping of the responses to the S1 stimuli indicated that the electrodes recorded activity within 20° from the visual field midline, that is, in parts of the visual field representations which are connected by axons of the corpus callosum (Innocenti et al. 2002; Manger et al. 2002). A custom made cryoloop 7 mm long and 2 mm wide, was centered on the 17/18 border of the left hemisphere. One cycle of 30 S1, S2, or S3 repetitions was performed at the baseline conditions. Then the cryoloop was cooled to 2 ± 1.5 °C. This procedure is known to deactivate all cortical layers under the probe (Lomber et al. 1999). After 5 min waiting meant to stabilize the temperature, another stimulation cycle was performed, followed by about 30 min recovery to baseline temperature after which a new stimulation cycle was performed.

LFPs were amplified by conventional amplifiers, digitized at 1 kHz (Plexon, Inc., Dallas, TX) and further filtered offline. We applied a notch filter at 50 Hz and locally weighted smoothing with least squares linear polynomial fitting to suppress high (above 120 Hz) and low (below 4 Hz) frequency noise.

Data Analysis

LFP responses to visual stimuli were processed as follows. We identified and eliminated about 5% of LFPs whose shape showed a strong deviation from the standard LFP profile (see Results) and which therefore where suspected of being artifactual.

For each class of stimuli we tested the null hypothesis that the stimulus-locked LFPs during cooling of the contralateral hemisphere did not differ from those under baseline and recovery conditions. We also tested whether LFPs during recovery differed from the baseline. We employed the multivariate analysis of variance whereby the voltage at each time sample is considered as a dependent variable (response) and factors are the categorical variables expressing the experimental condition, that is, baseline-cooling-recovery. This approach resulted in many highly correlated dependent variables (e.g., 150 variables for a 150 ms LFP sampled at 1 kHz), whose number far exceeds the number of observations (e.g., 10 observations for the 10 presentations of the S1 stimulus). In this case, classical multivariate analysis cannot be directly applied therefore we used a 50-50 multivariate analysis of variance (MANOVA) approach (Langsrud 2002). This approach first uses principal components (PCs) analysis to project data onto a new space defined by orthogonal axes that most efficiently describe the variation within the data. These axes are ordered according to how much of the variance of the original data they contain (Malinowski 1991). Most of the data dissimilarities between observations in different experimental conditions (baseline-cooling-recovery) will be captured by the first several PCs. In the simplest case the next step would be to use few PCs, which explain at least 75% of the variance in the data, for an ordinary MANOVA test. However, Langsrud (2002) showed that another strategy can enhance the power of the test. Namely, the first k PCs explaining 50% of the variability are used to calculate the model

prediction. The error is evaluated over the last 25% of all PCs. Then the classical MANOVA (F test with the significance level at $P = 0.05$) is applied on the ratio between the mean of the first 50% and the mean of the last 25% of PCs.

In the case of the S1 stimulus we had 10×10 positions to analyze. An indiscriminate use of the statistical test could result in an uncontrolled growth of Type I (false positive) errors. We address this multiple comparison problem by combination of the above described 50-50 MANOVA with control of False Discovery Rate (Benjamini and Hochberg 1995).

In addition to testing the null hypothesis as described above, for all LFPs we measured latencies, amplitudes and durations of LFP peaks. These values were further used for statistical assessments of 1) mean and standard deviation (SD) of LFP peaks, and 2) significance of the difference in the LFP amplitude among baseline and cooling conditions with ANOVA. To assess the latency of an LFP we used a method inspired by Kaur et al. (2004). We first calculated a baseline as the mean voltage recorded by an electrode during the first 20 ms after stimulus onset and preceding the rise of the LFP. A threshold line is then drawn, parallel to the baseline, and either below, or above it, depending on the polarity of the LFP considered. To avoid spurious crossing of the threshold line due to chance fluctuation of the signal we first chose a conservative threshold value which for a negative LFP is given by: $V_{thr} = V_{bline} - 3(V_{bline} - V_{min})$, where V_{bline} is the baseline voltage and V_{min} is the voltage minimum evaluated over the first 20 ms after stimulus onset. The initial phase of the LFP was approximated by a straight line starting from the baseline and tangent to the LFP. This tangent was calculated by fitting a straight line through 3 values of the LFP closest to the location of the intersection of the LFP with the threshold line. The intersection of the fitted line with the baseline gives a good robust estimate of the latency.

Results

Responses to the S1 Stimulus

We reconstructed the responses to 10×10 positions of the S1 stimulus at 45 electrode locations in 8 experiments. The responses (Fig. 2 and Supplementary Fig. 1) consisted of a LFP whose amplitude depended on stimulus location. Together, the LFPs delineated peripheral response fields (PRFs) consistent with the minimal response fields mapped with hand-moved stimuli while listening to spikes (as in Manger et al. 2002; Nakamura et al. Forthcoming). As expected, within the cortical territory covered by the multielectrodes, the positions of the PRFs changed, in azimuth and elevation according to the retinotopic maps of areas 17 and 18 (Manger et al. 2002). That is, the elevation of PRFs increased in the medial to lateral direction, and the azimuth decreased in the posterior to anterior direction up to a minimum, corresponding to the midline of the visual field at the 17/18 border and increased again in area 18 (Supplementary Fig. 1). When the eye misalignment induced by paralysis was uncompensated, 2 separate PRFs could be identified, 1 for each eye, with the largest responses usually evoked from the contralateral eye (Supplementary Fig. 1). The LFPs began at 24-37 ms with a tendency toward shorter latencies near the PRF center and longer latencies at the periphery (not shown) as in Nakamura et al. (Forthcoming). The first, negative component of the LFPs lasted between 80 and 120 ms; it was followed by a longer lasting positive component (see Nakamura et al. Forthcoming).

Cooling the contralateral hemisphere did not notably affect the responses to the S1 stimulus, and the subtraction of the responses before and during cooling resulted in essentially flat traces (Fig. 2). To test for possible minor changes, the data
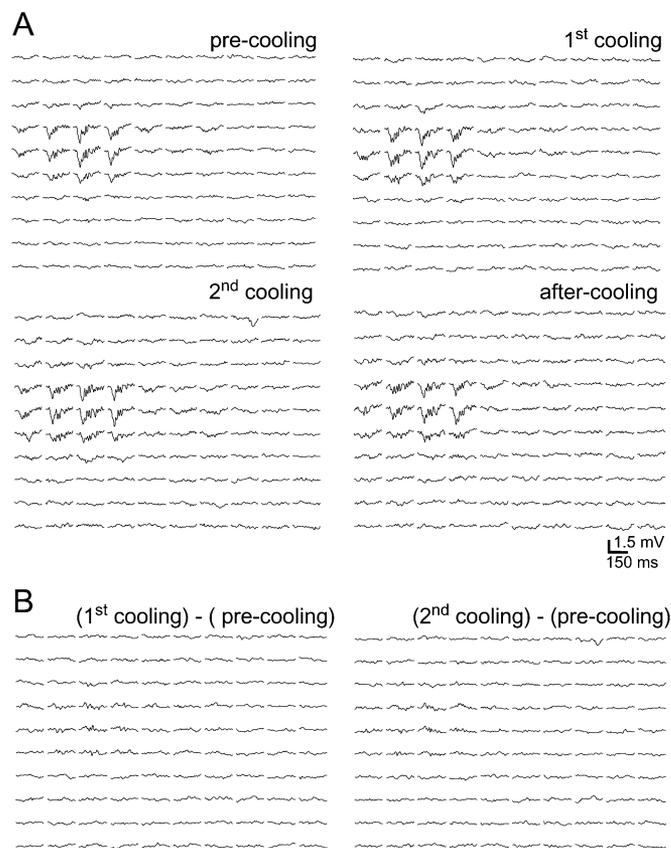

Figure 2. (A) Responses to stimulus S1 before, during and after 2 successive cooling sessions. At each position S1 generated LFPs of different amplitude, which together delineated a PRF (see also Supplementary Fig. 1). Neither the location of the PRFs nor the amplitude or shape of the LFPs was changed by cooling the contralateral hemisphere. (B) Subtractions of the responses obtained before cooling, from those obtained during the first and second cooling sessions. As expected, they are flat. In the same experiment and microelectrode location cooling elicited the D type response shown in Figure 4, during stimulation with the S2 grating.

were subjected to 50-50 MANOVA test applied separately to the LFPs recorded at each stimulus position. This analysis was performed on the responses recorded at 30 microelectrode locations for each of the 10×10 stimulus positions. Significant changes with cooling were seen at 58 out of the 479 stimulus locations which fell within the PRFs. However, most of these changes did not recover after cooling, and therefore might have been due to response variability rather than to suppressed callosal input. In addition, significant changes were also found outside the PRFs in a significant number of cases (152 in 2521). Finally, when we used the False Discovery Rate method to control for Type I error only 4 of the 58 responses within the PRFs, still maintained significant changes with cooling.

In conclusion, the input from the contralateral visual areas does not contribute significantly, if at all, to the PRFs mapped with discrete stimuli flashed near the visual field midline, as also suggested by previous work (Nakamura et al. Forthcoming). Discrete, short-lasting stimuli appear not to be processed through interhemispheric interactions in the primary visual areas.

Responses to the S2 Stimulus

We recorded responses to the S2 stimulus at 107 microelectrode locations in 9 experiments, and at each location, for 8

orientations and directions of motion of the gratings. The majority of the responses consisted of 2 negative waves (Fig. 3). The first, larger wave corresponded to the presentation of the static stimul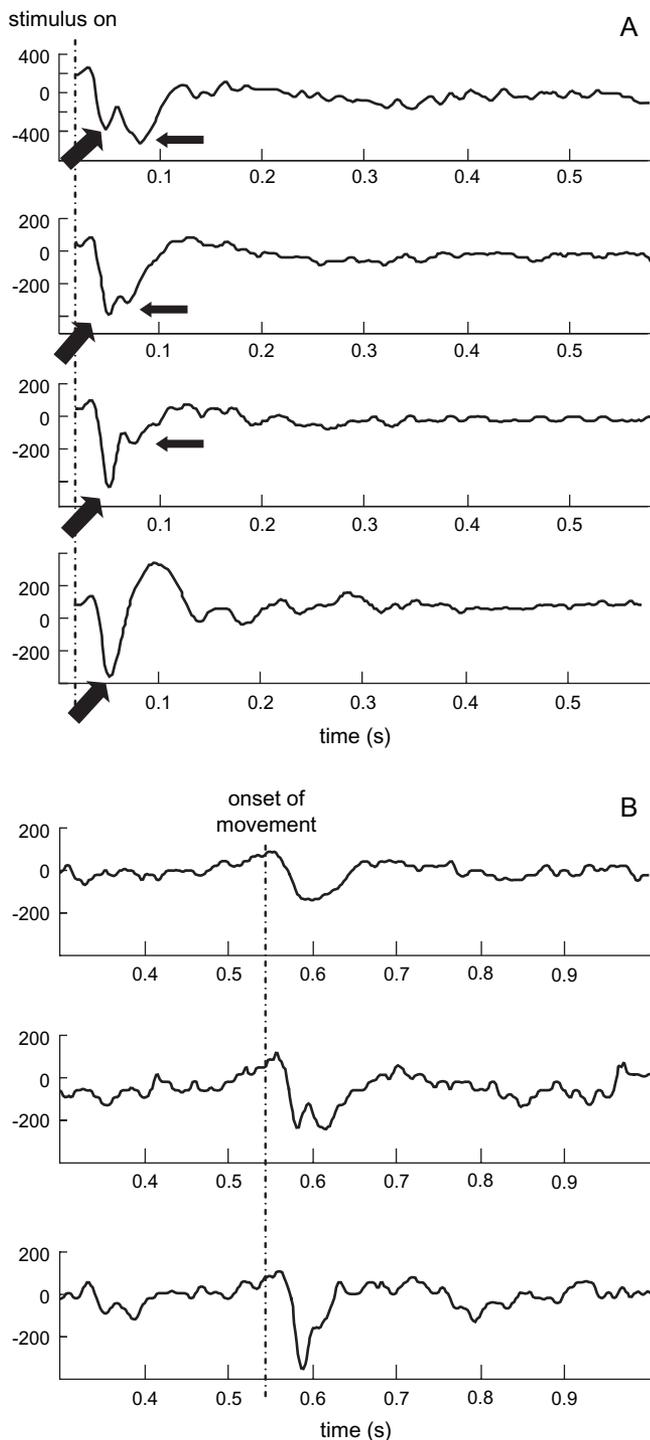us and consisted, in most cases (63%), of 2 peaks here from called N1 and N2. On average, N1 started at 23.0 (±6.8 SD) ms after stimulus onset, peaked at 36.3 (±11.0) ms, and lasted for 25.0 (±8.4) ms. N2 originated in the falling phase of N1, it peaked at 60.9 (±12.2) ms and lasted 56.8 (±20.6) ms. The amplitude of both N1 (-242.8 μV ± 230.3 SD) and N2 (-148.9 μV ±110.0 SD) varied across experiments and N2 could occasionally be absent. The second negative wave evoked by the S2 stimulus occurred 53.2 ±48.3 SD ms after the onset of stimulus motion and we shall refer to as dynamic negative response (DN). It usually consisted of a single, negative wave peaking at 73.4 (±43.8 SD) ms after onset of motion, lasting 54.1 (±30.9 SD) ms. The DN peak was smaller than the response to the static stimulus (-81.9 μV ± 69.5 SD), more variable in its amplitude and shape, and sometimes absent (Fig. 3).

The amplitude of N1 and N2 varied somewhat with stimulus orientation although this might be due to the position of the contrasts on the PRFs, rather than to the orientation of the gratings. The variability of the DN LFPs discouraged the analysis of their orientation specificity.

Cooling the contralateral hemisphere significantly affected the amplitudes of N1 and/or N2 peaks in 52% of 640 LFPs. After cooling, the responses fully recovered to levels statistically indistinguishable from baseline in 27% of the cases ($P < 0.05$), incompletely ($P < 0.125$) in another 12% of cases. The 39% of responsive LFPs which recovered fully or partially after cooling will be described together (Figs 4 and 5A and Table 1). Those
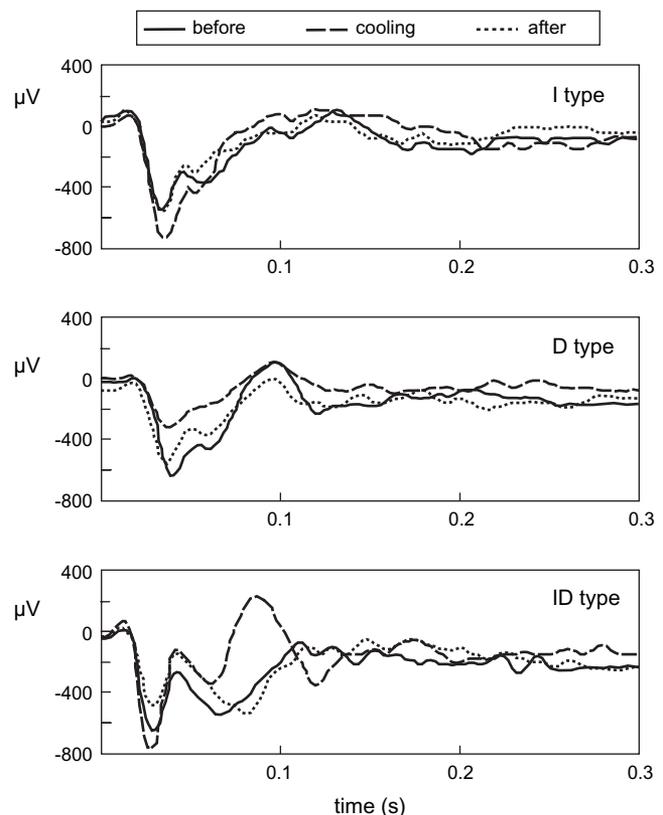

Figure 3. Types of LFPs obtained with the S2 or S3 stimuli. Stimuli invariably generated an LFP response when appearing in the visual field (response to static stimulus (A) and less constantly a longer latency, lower amplitude response initiated by stimulus motion (response to dynamic stimulus (B). The static response usually had 2 peaks at different latencies (arrows) but the second peak could vary in amplitude and was occasionally absent. The response to the dynamic stimulus was usually 1 peak (as in the uppermost example) but occasionally 2 peaks were also seen.

Figure 4. Cooling the contralateral hemisphere modifies the responses to the stimuli (examples from S2 stimuli). Cooling either increased (I type effect) or decreased (D type effect) the amplitude of the response although sometimes the effects were more complex and depended on latency after stimulus onset. For example, in the recording from experiment 041105 (electrode CH 4; bottom panel) statistical analysis shows a moderate increase of the static response, first peak at 24–40 ms and a more robust decrease of the second peak at 60–80 ms (ID effect).
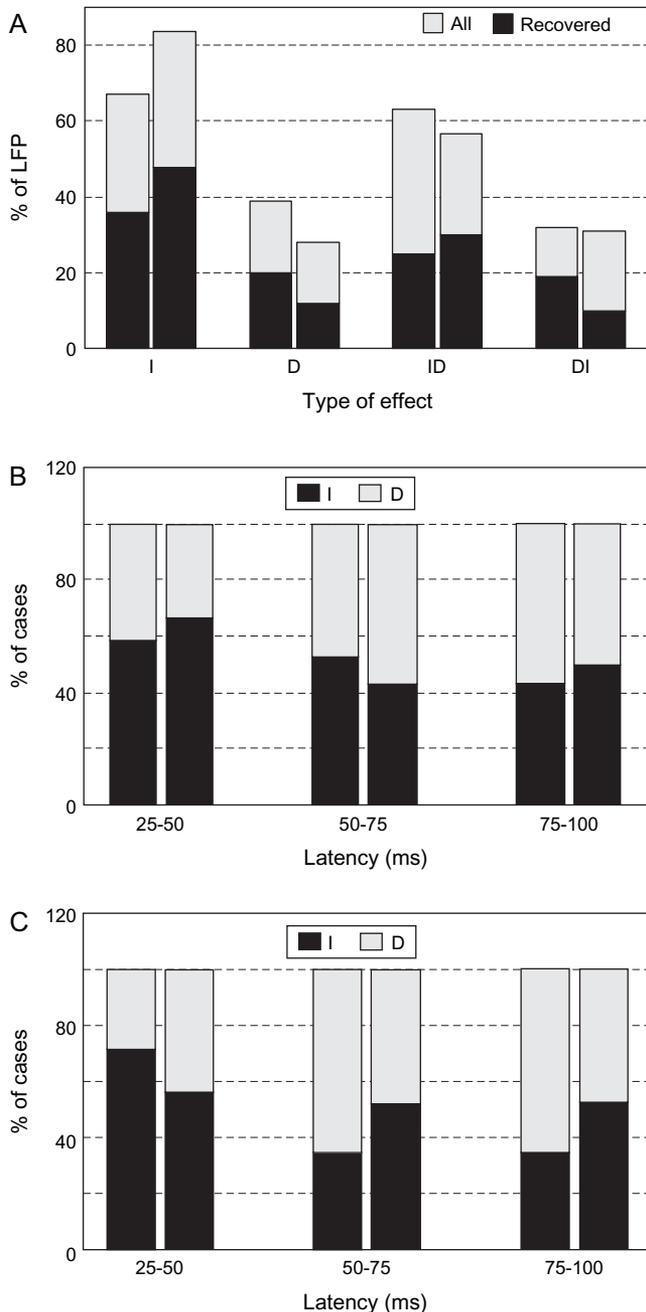
Figure 5. (*A*) Frequency of cooling effects on the responses to the static phase of S2 (left bars in each pair) and S3 (right bars) stimuli. I: increase in response amplitude, D: decrease in response amplitude, ID: sequence of increase–decrease, and DI: sequence of decrease–increase. Notice that I and ID predominate both with S2 and with S3 and that the distribution of effects is similar for the LFPs which recovered after cooling and for those which did not. (*B,C*) Latency of the I and D effects for the static phase of S2 (left bars) and S3 (right bars) stimuli; responses recovered after cooling (*B*) and all responses (*C*). The 2 panels consistently show a higher frequency of increase in the early phase of the responses and a progressively more frequent decrease at longer latencies.

Table 1

Magnitude (left 3 columns, in percent of precooling values) and frequency (right 2 columns; in percent of total cases) of changes caused by cooling during the presentation of S2 and S3 stimuli

S2

	N1 amplitude	N2 amplitude	DN amplitude	Static	Dynamic
I	**36.83**	**40.37**	**57.32**	36	63
D	−24.69	**−45.38**	**−38.10**	20	37
ID	**34.12**	−17.29		25	
DI	−29.25	31.29		19	
Totals increase static: 36 + 25 = 61			dynamic: 63		
Totals decrease static: 20			dynamic: 37		

S3

	N1 amplitude	N2 amplitude	DN amplitude	Static	Dynamic
I	**79.92**	**63.40**	*47.10*	48	38
D	**−27.35**	**−34.06**	**−43.97**	12	62
ID	**105.07**	**−35.87**		30	
DI	**−48.53**	**154.83**		10	
Totals increase static: 48 + 30 + 10 = 88			dynamic: 38		
Totals decrease static: 30 + 10 = 40			dynamic: 62		

Note: The significant values are in bold. Nonsignificant values are in italics. The cumulative frequency of the increases and of decreases is also shown. Data are from cases which recovered after cooling. Notice that the data seem to show a larger increase in the N1 and N2 responses with cooling for the S3 than for the S2 stimuli. But these were not confirmed when the unrecovered cases were also analyzed.

with no recovery were considered ambiguous and, we shall not describe them in detail.

In 36% of the recovered cases either N1 or N2 or both were increased during cooling (the I effect; Figs 4 and 5*A* and Table 1) to, respectively, 37% and 40% of baseline on average. In 20% of cases either N1 or N2 or both were decreased (the D effect; Figs 4 and 5*A* and Table 1), but the decrease of N1 did not reach statistical significance, whereas that of N2 (–45% of baseline) did. In 25% of the responsive LFPs N1 was increased and N2 decreased (the ID effect; Figs 4 and 5*A* and Table 1) but only the increase of N1 (34%) was statistically significant. Finally, in 19% of the cases N1 decreased and N2 increased (the DI effect). The decrease in N1 did not reach significance, whereas the increase of N2 was significant only in the cases with full recovery (Fig. 5*A* and Table 1).

In conclusion, during the static phase of stimulus presentation both N1 and N2 significantly increased during cooling whereas only N2 decreased. Globally, the increase was more frequently observed than the decrease (61 vs. 20 cases; Table 1).

The effects of cooling the contralateral hemisphere on the responses to moving gratings, the DN responses, could be studied in 547 LFPs. Cooling significantly affected 22% of the cases, of which 60% recovered to the $P < 0.05$ criterion and 63% to the $P < 0.125$ criterion. Among these, the I effect was more frequent (63%) and larger (57% of baseline), than the D effects (37% and –37%, respectively) (Fig. 6 and Table 1).

Therefore, when iso-oriented moving gratings are shown to the 2 hemispheres, they either facilitate or depress each other's response, but the latter seems to predominate in both frequency and amplitude.

Responses to the S3 Stimulus

We recorded responses to the S3 stimulus to test if the interaction between the hemispheres depended on whether they processed identical or different stimuli with, for example, iso-oriented columns in the 2 hemispheres interacting differently from the orthogonally oriented ones.

We recorded the responses to the S3 stimulus at 81 microelectrode locations in 8 experiments, for 8 orientations and direction of motions (Fig. 1). As for S2, both the appearance
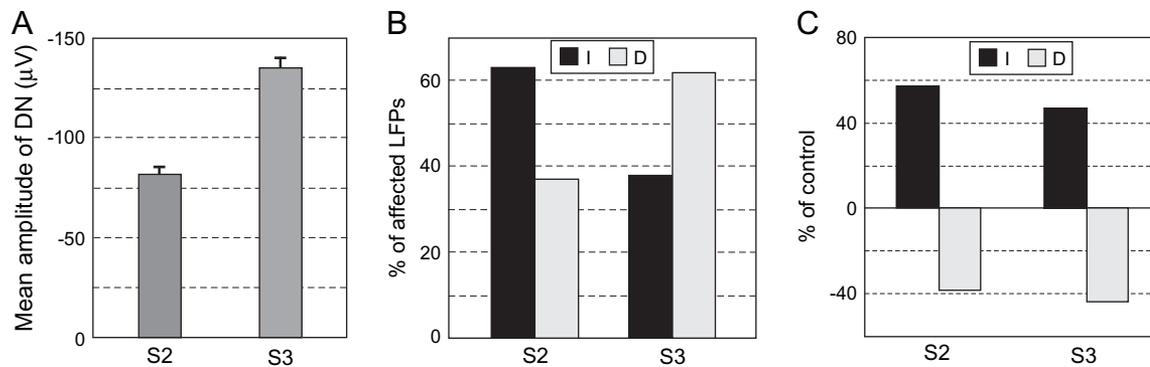
Figure 6. (*A*) Mean amplitude and the standard error of the dynamic phase of the response to S2 and S3 stimuli. (*B*) Frequency and (*C*) magnitude of cooling effects on the dynamic phase of the responses to S2 and S3. Notice that the response to the dynamic phase of the stimuli consisted of a negative wave, of larger amplitude for S3 than for S2. Instead, the amplitude of the responses to the static phase of the S2 and S3 stimuli (not shown; see text) was not different. Cooling more often increased (I) the amplitude of the response to S2 and decreased (D) that to S3. Also, the increase was larger than the decrease for the S2 stimuli. For the S3 stimuli the opposite was true; furthermore, the increase was not statistically significant when only the responses which fully recovered after cooling were considered. Only the cases which recovered after cooling are shown (Table 1).

of the static stimulus and the onset of stimulus movement evoked potentials with features similar to those elicited by S2. N1 latency was 22.1 ms (±5.9 SD), time to peak 29.3 ms (±8.6 SD), duration 18.8 ms (±8 SD), and amplitude −226.1 μV (±238.4 SD). N2 peaked at 58.9 ms (±18.6 SD), lasted 53.8 ms (±21.4 SD) and its amplitude was −159.8 μV (±155.8 SD).

After cooling, the responses recovered to levels statistically indistinguishable from baseline in 21% of cases ($P < 0.05$), incompletely ($P < 0.125$) in another 7% of cases. As for S2, both I, D, ID, and DI effects could be identified (Fig. 5*A* and Table 1). The I effect was observed in 48% of the responsive and recovered LFPs with a significant increase of 80% of N1 and 63% of N2. The D effect was found in 12% of the recovered LFPs but was statistically insignificant. The ID effect was observed in 30% of the LFPs with significant increases of N1 to 105% of baselines and decreases of N2 to −35.9. Finally, DI was observed in 10% of cases with N1 significantly decreasing to −49% of baseline and N2 increasing to 155% of baseline levels. Globally, the increase was more frequently observed than the decrease (88 vs. 44 cases; Table 1).

These findings concur with those obtained with the S2 in demonstrating that gratings extending over both hemifields are processed by interhemispheric interaction, and this processing more frequently depresses the responses elicited through the thalamo-cortical pathway.

The effects of cooling the contralateral hemisphere on the responses to moving gratings, the DN responses, could be studied in 24% of LFPs (Fig. 6 and Table 1). Latency (43.2 ms ± 26.0 SD), peak position (74.7 ms ± 14.0 SD), and duration (51.7 ms ± 28.8 SD) were similar to those elicited by S2. However, the amplitude was significantly ($P < 10^{-4}$) greater than that elicited by the S2 stimulus (−135.3 μV ± 93.5 SD). Cooling affected 37% of the cases with full recovery and 13% more of cases with incomplete recovery (Fig. 6). Among these, the D effects predominated (62%), over the I effects (38%). Interestingly, only the D effects reached statistical significance in the sample of recovered LFPs (−43.9%), whereas the I effect reached significance only in the full sample of recovered and not-recovered LFPs, (not shown) where its magnitude (28.1%) remained, however, inferior to that of the D effect (−35.6%).

Therefore, when different moving gratings are shown to the 2 hemispheres, they either facilitate or depress each other's response, but unlike in the case of iso-oriented gratings, the first seems to predominate in both frequency and amplitude.

Latency of the Interhemispheric Interactions

To study the latency of the interactions between the hemispheres, the effects of cooling on the responses elicited by the static phase of S2 and S3 stimuli were broken down into 3 time bins covering 25–50, 50–75, 75–100 ms after stimulus onset (Fig. 5*B*,*C*). The 3 bins cover the most significant dynamics of the response to the static stimulus where we usually observed 2 peaks (Fig. 3) and 4 different types of cooling effect (Fig. 5*A*). For both S2 and S3 static stimuli, the I effects occurred predominantly at the shortest latencies after the stimulus onset, whereas the D effects became progressively more frequent with increasing latency. This may indicate that the depressing interactions between the hemispheres is conducted through faster pathways that the facilitating interactions.

Discussion

Methodological Considerations

We have analyzed hemispheric interactions by recording LFPs because they provide a "mesoscopic" level of spatial resolution between the previously used (see Introduction) electroencephalography signal and the single units. In addition, because the LFPs reflect the depolarization of neuronal membranes rather than firing, they are more sensitive than single unit recordings and more directly comparable with the results obtained in parallel with optical imaging and voltage sensitive dye (Schmidt et al. 2005; Nakamura et al. Forthcoming).

The inactivation of the visual cortex by cooling was introduced by Payne et al. (1991) in studies of interhemispheric interactions similar to those reported here and was later extended to other studies (e.g., Lomber et al. 1994; Galuske et al. 2002). Compared with callosal transection, it has the following advantages. It is less invasive. The effects are reversible and studying the responses both before and after inactivation of the other hemisphere, eliminates the confounding effects of spontaneous trends in neuronal responsiveness.

In split-chiasm preparations (Berlucchi and Rizzolatti 1968; reviewed in Ptito 2003) the responses to the stimulation of the contralateral eye unmask the callosal input. However, days of recovery after the split-chiasm operation are usually required, which can cause rearrangements of connectivity or synaptic strength. Also, the study is restricted to the neurons fed by temporal retina. The callosal interactions involving the nasal retina, which in the ferret provides the majority of the retinofugal afferents, cannot be evaluated. Cooling one hemisphere does not interrupt callosal fibers, but the anatomy of the visual pathways leaves little doubt that it highlights the influence of its callosal projection to the other hemisphere. Finally, the fact that cooling selectively affected the responses to gratings, not those to flashing squares speaks, against unspecific effects, in particular the possibility that cooling might have directly affected the recorded hemisphere (Payne et al. 1991; Lomber et al. 1994, 1999).

A Model of Interhemispheric Interaction in the Visual Areas

Four results of the present study are worth emphasizing.

First, the input from the contralateral hemisphere appears not to be relevant to location, size, shape, and response strength of the PRFs mapped by flashing stimuli of short duration near the visual field midline. This finding confirms what was reported in the companion paper (Nakamura et al. Forthcoming).

Second, eliminating input from the contralateral hemisphere does not suppress responses to the visual stimulus, but modifies them in a complex manner. Therefore, callosal input in areas 17 and 18, mainly cooperates with the thalamo-cortical input which it modifies. This might be a common principle of callosal function, because it also applies to the somatosensory areas in cats, humans, and rodents (Innocenti et al. 1973; Fabri et al. 2006; Li and Ebner 2006). This modulatory role of callosal connections is consistent with the morphology of callosal axons reported in the cat (Tettoni et al. 1998) and with the modest size of most of the excitatory postsynaptic potentials elicited by transcallosal stimuli in somatosensory, visual and association areas of the cat (Innocenti et al. 1972; Toyama et al. 1974; Cissé et al. 2003). This is also in line with the evidence, that the same connections develop under the control of thalamically mediated visual input (reviewed in Innocenti and Price 2005).

Third, LFP responses elicited by gratings depend on input from the corresponding areas of the contralateral hemisphere and the effects are stimulus-specific. Most striking were the different effects on the dynamic phase of the S2 and of the S3 stimuli. Sixty-three percent of the responses to S2 were increased by cooling and 37% decreased, whereas with the S3 stimulus 38% of the responses increased and 62% decreased. The increase with cooling of the responses to the S2 gratings might be due to release from callosally driven iso-orientated inhibitions (Ferster 1986; Kisvárday et al. 1994; Monier et al. 2003). Instead, the decrease of the response to the S3 gratings might be due to the fact that S3 stimuli activate different sets of orientation and/or direction specific neurons via the thalamo-cortical and via the callosal routes. Cooling eliminates the latter, hence reducing the responses.

Fourth, both excitatory and inhibitory input from the contralateral visual areas can be inferred from the effects of cooling. The inhibitory effect predominated at short (25–50 ms)

latencies after stimulus onset, the excitatory effect at longer latencies (≥50 ms). The latencies of both effects are compatible with callosal conductions (below).

Our results resemble those obtained with similar inactivation techniques by Payne et al. (1991) on single neurons in that contralateral inactivation both increased (46%) and decreased (41%), the responses (the rest being unaffected) (see also Kitzes and Doherty 1994 for similar results with auditory callosal connections in the ferret).

Examples of both excitatory and inhibitory interactions between the hemispheres go far back in the literature (reviewed in Innocenti 1986; Anninos and Cook 1988) and whether one or the other prevails has fueled an old debate (reviewed in Bloom and Hynd 2005). Clearly in the visual areas, both effects were found; which prevails depends on stimulus configuration and phase of the response.

Figure 7 models the main aspects of the present results. The fact that the responses to gratings but not those to small flashing stimuli are affected by inactivating the contralateral hemisphere indicates that interhemispheric interactions
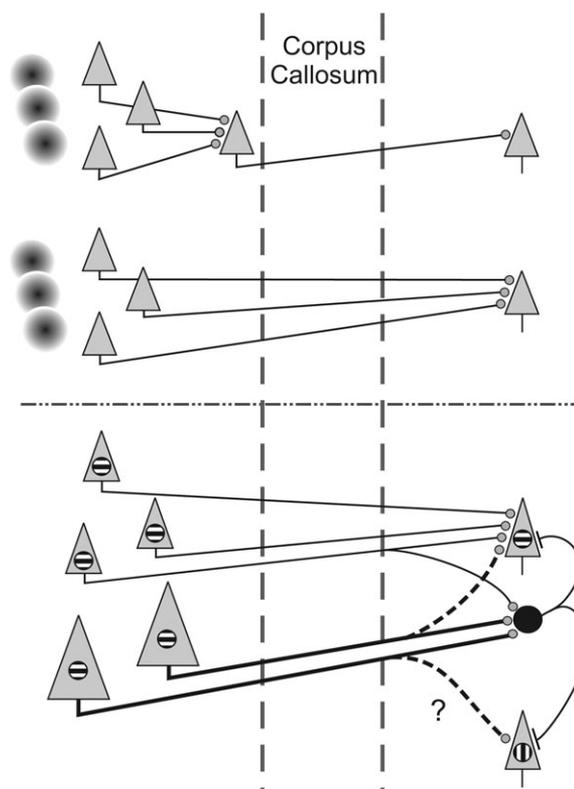

Figure 7. A model meant to capture the main aspects of the present results. Upper panel: because small squares do not affect contralateral targets, whereas gratings do, it appears that the output from neurons responsive to the small squares needs summation, to affect the contralateral targets. The cartoon suggests that the summation can occur either at the output stage of the sending hemisphere or at the target neurons in the receiving hemisphere. Lower panel: the interhemispheric input appears to be mainly excitatory (round synaptic axonal terminals), however, it elicits an early inhibitory response, via local interneurons. This early inhibition is more widespread than the excitation and might be driven mainly via thicker axons, with higher conduction velocity, whereas the later excitation is driven mainly by thinner, lower conduction velocity axons. The lower panel captures the following additional aspects of the results: inhibition is both between iso-oriented and cross-oriented neurons. Excitation is mainly between iso-oriented neurons. There may be an early, but weak iso-oriented and cross-oriented (question mark) excitation (interrupted lines). For further discussion see text.

require spatial summation. The summation might occur on the callosally projecting neurons. Indeed, in the cat, some of these neurons have "simple" receptive fields, best activated by elongated stimuli (Berlucchi et al. 1967; Hubel and Wiesel 1967; Shatz 1977; Innocenti 1980). However, they are a minority of the callosally projecting neurons (between 7% and 13%; Shatz 1977; Innocenti 1980; McCourt et al. 1990). Therefore, summation might occur at the target neurons, most of which appear to have receptive fields of the "complex" type (Berlucchi et al. 1967; Innocenti 1980; Lepore and Guillemot 1982; McCourt et al. 1990).

Figure 7 assumes that mainly neurons responding to the same stimulus orientation are interconnected by excitatory callosal axons. This conforms to the majority of the experimental evidence to date (Schmidt et al. 1997; Kiper et al. 1999; Rochefort et al. 2007). Callosal connections are excitatory but cause inhibition via an interneuron, as shown by most studies (reviewed in Innocenti 1986; see also Cissé et al. 2003; Karayannis et al. 2007), although a few direct inhibitory connections exist between the hemispheres (Peters et al. 1990; Fabri and Manzoni 1996). We also assume that the inhibitory interneurons driven by a given orientation contact both iso-oriented and non–iso-oriented neurons (Kisvárday et al. 1994; Monier et al. 2003; Mariño et al. 2005).

Because inhibitory interactions predominate, at short latencies, and excitatory interactions at longer latencies after the stimulus, the model assumes that thicker and fast conducting callosal axons cause inhibition by contacting interneurons, whereas the slower excitatory connections are mainly excitatory. This is consistent with a previous model of callosal interactions in the visual areas whereby time differences between excitatory and inhibitory interactions could modulate the oscillatory cycles of the hemispheres (Innocenti et al. 1995). Indeed, the corpus callosum contains a large spectrum of axon diameters (Berbel and Innocenti 1988; LaMantia and Rakic 1990) some of which (0.25–3 μm; light microscopic material) originating from the border between areas 17 and 18 (Houzel et al. 1994), which was the target of the present study. Measured conduction velocity at the 17/18 border of the cat range between 1.4–27 or 8–30 m/s (in different studies) and orthodromic conduction delays between 2 and 20 ms (reviewed in Innocenti et al. 1995).

Some Relevant Findings from Split-Brain Studies

In a famous study (Ramachandran et al. 1986), small (20 min of arc) stimuli of short duration (130 ms) were flashed in succession within or across hemifields in normal and split-brain subjects. As it was discussed elsewhere (Nakamura et al. Forthcoming), the differences in the across-hemifield condition versus within hemifield conditions at certain interstimulus intervals presentations (Ramachandran et al. 1986; Naikar and Corballis 1996) do not need to be explained by interhemispheric interactions.

In contrast, our finding that the responses to gratings extending in the 2 hemifields is modified after cooling of the contralateral visual areas seems compatible with the finding that 2 split-brain patients could judge correctly the alignment of line segments flashed separately in the 2 hemifields, although with a deficit, compared with the presentation in either hemifield (Corballis 1995). This deficit stresses the role of corticocortical connections in integrating line segments across

the visual field although callosal connections may be less efficient than the intra-areal connections (Pillow and Rubin 2002).

Conclusions

The visual areas 17 and 18 of the 2 hemispheres interact in 3 different ways. Interactions 1) modulate the amplitude of the responses to a visual stimulus in the complex ways described here; 2) modify the synchronization of the responses, of the 2 hemispheres (Engel et al. 1991; Munk et al. 1995; Kiper et al. 1999; Knyazeva et al. 2006; Rose et al. 2006); and 3) modulate the formation of stimulus-driven synchronous neuronal assemblies in each hemisphere (Carmeli et al. 2007). These interactions are stimulus-specific. They depend on which stimulus the hemispheres "see" and whether they are the same or different; therefore they can contribute to stimulus detection and/or categorization. This may be achieved by increasing signal-to-noise ratio to certain stimuli, in particular to identical and coherent stimuli in the 2 hemifields. Consistent with this, orientation-specific responses to full-field gratings recorded by imaging intrinsic optical signal is attenuated by inactivating the contralateral areas (Schmidt et al. 2005).

References

Anninos PA, Cook ND. 1988. Neural net simulation of the corpus callosum. Int J Neurosci. 38:381–391.

Antonini A, Berlucchi G, Lepore F. 1983. Physiological organization of callosal connections of a visual lateral suprasylvian cortical area in the cat. J Neurophysiol. 49:902-921.

Benjamini Y, Hochberg Y. 1995. Controlling the false discovery rate: a practical and powerful approach to multiple testing. J Roy Stat Soc Ser B. 57:289–300.

Berbel P, Innocenti GM. 1988. The development of the corpus callosum in cats: a light- and electron-microscopic study. J Comp Neurol. 276:132-156.

Berlucchi G. 1972. Anatomical and physiological aspects of visual functions of corpus callosum. Brain Res. 37:371-392.

Berlucchi G, Gazzaniga MS, Rizzolatti G. 1967. Microelectrode analysis of transfer of visual information by the corpus callosum. Arch Ital Biol. 105:583-596.

Berlucchi G, Rizzolatti G. 1968. Binocularly driven neurons in visual cortex of split-chiasm cats. Science. 159:308-310.

Bloom JS, Hynd GW. 2005. The role of the corpus callosum in interhemispheric transfer of information: excitation or inhibition? Neuropsychol Rev. 15:59-71.

Carmeli C, Knyazeva MG, Innocenti G, De Feo O. 2005. Assessment of EEG synchronization based on state-space analysis. Neuroimage. 25:339-354.

Carmeli C, Lopez-Aguado L, Schmidt K, De Feo O, Innocenti GM. 2007. A novel interhemispheric interaction: modulation of neuronal cooperativity in the visual areas. PloSONE.

Cissé Y, Grenier F, Timofeev I, Steriade M. 2003. Electrophysiological properties and input-output organization of callosal neurons in cat association cortex. J Neurophysiol. 89:1402-1413.

Corballis MC. 1995. Visual integration in the split brain. Neuropsychologia. 33:937-959.

Engel AK, König P, Kreiter AK, Singer W. 1991. Interhemispheric synchronization of oscillatory neuronal responses in cat visual cortex. Science. 252:1177-1179.

Fabri M, Manzoni T. 1996. Glutamate decarboxylase immunoreactivity in corticocortical projecting neurons of rat somatic sensory cortex. Neuroscience. 72:435-448.

Fabri M, Polonara G, Mascioli G, Paggi P, Salvolini U, Manzoni T. 2006. Contribution of the corpus callosum to bilateral representation of the trunk midline in the human brain: an fMRI study of callosotomized patients. Eur J Neurosci. 23:3139-3148.

Ferster D. 1986. Orientation selectivity of synaptic potentials in neurons of cat primary visual cortex. J Neurosci. 6:1284-1301.

Galuske RA, Schmidt KE, Goebel R, Lomber SG, Payne BR. 2002. The role of feedback in shaping neural representations in cat visual cortex. Proc Natl Acad Sci USA. 99:17083-17088.

Guillemot J-P, Paradis M-C, Samson A, Ptito M, Richer L, Lepore F. 1993. Binocular interaction and disparity coding in area 19 of visual cortex in normal and split-chiasm cats. Exp Brain Res. 94:405-417.

Houzel J-C, Milleret C, Innocenti G. 1994. Morphology of callosal axons interconnecting areas 17 and 18 of the cat. Eur J Neurosci. 6:898-917.

Hubel DH, Wiesel TN. 1967. Cortical and callosal connections concerned with the vertical meridian of visual fields in the cat. J Neurophysiol. 30:1561-1573.

Innocenti GM. 1980. The primary visual pathway through the corpus callosum: morphological and functional aspects in the cat. Arch Ital Biol. 118:124-188.

Innocenti GM. 1986. General organization of callosal connections in the cerebral cortex. In: Jones EG, Peters A, editors. Cerebral cortex, Vol. 5. New York: Plenum. p. 291-353.

Innocenti GM, Aggoun-Zouaoui D, Lehmann P. 1995. Cellular aspects of callosal connections and their development. Neuropsychologia. 33:961-987.

Innocenti GM, Manger PR, Masiello I, Colin I, Tettoni L. 2002. Architecture and callosal connections of visual areas 17,18,19 and 21 in the ferret (Mustela putorius. Cereb Cortex. 12: 411-422.

Innocenti GM, Manzoni T, Spidalieri G. 1972. Peripheral and trans-callosal reactivity of neurones within SI and SII cortical areas. Segmental divisions. Arch Ital Biol. 110:415-443.

Innocenti GM, Manzoni T, Spidalieri G. 1973. Relevance of the callosal transfer in defining the peripheral reactivity of somesthetic cortical neurones. Arch Ital Biol. 111:187-221.

Innocenti GM, Price DJ. 2005. Exuberance in the development of cortical networks. Nat Rev Neurosci. 6:955-965.

Karayannis T, Huerta-Ocampo I, Capogna M. 2007. GABAergic and pyramidal neurons of deep cortical layers directly receive and differently integrate callosal input. Cereb Cortex. 17: 1213-1226.

Kaur S, Lazar R, Metherate R. 2004. Intracortical pathway determine breadth of subthreshold frequency receptive fields in primary auditory cortex. J Neurophysiol. 91:2551-2567.

Kiper DC, Knyazeva MG, Tettoni L, Innocenti GM. 1999. Visual stimulus-dependent changes in interhemispheric EEG coherence in ferrets. J Neurophysiol. 82:3082-3094.

Kisvárday ZF, Kim D-S, Eysel UT, Bonhoeffer T. 1994. Relationship between lateral inhibitory connections and the topography of the orientation map in cat visual cortex. Eur J Neurosci. 6: 1619-1632.

Kitzes LM, Doherty D. 1994. Influence of callosal activity on units in the auditory cortex of ferret (Mustela putorius). J Neurophysiol. 71:1740-1751.

Knyazeva MG, Fornari E, Meuli R, Innocenti G, Maeder P. 2006. Imaging a synchronous neuronal assembly in the human visual brain. Neuroimage. 29:593-604.

Knyazeva MG, Kiper DC, Vildavsky VJ, Despland PA, Maeder-Ingvar M, Innocenti GM. 1999. Visual stimulus-dependent changes in interhemispheric EEG coherence in humans. J Neurophysiol. 82:3095-3107.

LaMantia A-S, Rakic P. 1990. Cytological and quantitative characteristics of four cerebral commissures in the rhesus monkey. J Comp Neurol. 291:520-537.

Langsrud O. 2002. 50-50 multivariate analysis of variance for collinear responses. The Statistician. 51:305-317.

Lepore F, Guillemot J-P. 1982. Visual receptive field properties of cells innervated through the corpus callosum in the cat. Exp Brain Res. 46:413-424.

Li L, Ebner F. 2006. Balancing bilateral sensory activity: callosal processing modulates sensory transmission through the contralateral thalamus by altering response threshold. Exp Brain Res. 172:397-415.

Lomber SG, Cornwell P, Sun J-S, MacNeil MA, Payne BR. 1994. Reversible inactivation of visual processing operations in middle suprasylvian cortex of the behaving cat. Proc Natl Acad Sci USA. 91:2999-3003.

Lomber SG, Payne BR, Horel JA. 1999. The cryoloop: an adaptable reversible cooling deactivation method for behavioral or electrophysiological assessment of neural function. J Neurosci Methods. 86:179-194.

Malinowski ER. 1991. Factor analysis in chemistry, 2nd ed.. New York: John Wiley & Sons.

Manger PR, Kiper D, Masiello I, Murillo L, Tettoni L, Hunyadi Z, Innocenti GM. 2002. The representation of the visual field in three extrastriate areas of the ferret (Mustela putorius) and the relationship of retinotopy and field boundaries to callosal connectivity. Cereb Cortex. 12:423-437.

Mariño J, Schummers J, Lyon DC, Schwabe L, Beck O, Wiesing P, Obermayer K, Sur M. 2005. Invariant computations in local cortical networks with balanced excitation and inhibition. Nat Neurosci. 8:194-201.

McCourt ME, Thalluri J, Henry GH. 1990. Properties of area 17/18 border neurons contributing to the visual transcallosal pathway in the cat. Vis Neurosci. 5:83-98.

Milleret C, Houzel J-C. 2001. Visual interhemispheric transfer to areas 17 and 18 in cats with convergent strabismus. Eur J Neurosci. 13:137-152.

Milleret C, Houzel JC, Buser P. 1994. Pattern of development of the callosal transfer of visual information to cortical areas 17 and 18 in the cat. Eur J Neurosci. 6:193-202.

Monier C, Chavane F, Baudot P, Graham LJ, Frégnac Y. 2003. Orientation and direction selectivity of synaptic inputs in visual cortical neurons: a diversity of combinations produces spike tuning. Neuron. 37:663-680.

Munk MHJ, Nowak LG, Nelson JI, Bullier J. 1995. Structural basis of cortical synchronization. II. Effects of cortical lesions. J Neurophysiol. 74:2401-2414.

Naikar N, Corballis M. 1996. Perception of apparent motion across the retinal midline following commissurotomy. Neuropsychologia. 34:297-309.

Nakamura H, Chaumon M, Kljin F, Innocenti GM. Forthcoming. Dynamic properties of the representation of the visual field midline in the primary visual areas of the ferret (Mustela Putorius). Cereb Cortex.

Payne BR, Siwek DF, Lomber SG. 1991. Complex transcallosal interactions in visual cortex. Vis Neurosci. 6:283-289.

Peters A, Payne BR, Josephson K. 1990. Transcallosal non-pyramidal cell projections from visual cortex in the cat. J Comp Neurol. 302:124-142.

Pillow J, Rubin N. 2002. Perceptual completion across the vertical meridian and the role of early visual cortex. Neuron. 33:805-813.

Ptito M. 2003. Functions of the corpus callosum as derived from split-chiasm studies in cats. In: Zaidel E, Iacoboni M, editors. The parallel brain: the cognitive neuroscience of the corpus callosum. Cambridge (MA): Massachusetts Institute of Technology Press. p. 139-153.

Ramachandran VS, Cronin-Golomb A, Myers JJ, et al. 1986. Perception of apparent motion by commissurotomy patients. Nature. 320:358-359.

Rochefort NL, Buzás P, Kisvárday ZF, Eysel UT, Milleret C. 2007. Layout of transcallosal activity in cat visual cortex revealed by optical imaging. Neuroimage. 36:804-821.

Rose M, Sommer T, Büchel C. 2006. Integration of local features to a global percept by neural coupling. Cereb Cortex. 16:1522-1528.

Schmidt KE, Kim D-S, Singer W, Bonhoeffer T, Löwel S. 1997. Functional specificity of long-range intrinsic and interhemispheric connections in the visual cortex of strabismic cats. J Neurosci. 17:5480-5492.

Schmidt KE, Lomber SG, Innocenti GM. 2005. Impact of interhemispheric connections on orientation preference maps in areas 17 and 18 of the ferret. Soc Neurosci. [Abstr. 508.13].

Shatz C. 1977. Abnormal interhemispheric connections in the visual system of Boston Siamese cats: a physiological study. J Comp Neurol. 171:229-246.

Tettoni L, Gheorghita-Baechler F, Bressoud R, Welker E, Innocenti GM. 1998. Constant and variable of axonal phenotype in cerebral cortex. Cereb Cortex. 8:543-552.

Toyama K, Matsunami K, Ohno T, Tokashiki S. 1974. An intracellular study of neuronal organization in the visual cortex. Exp Brain Res. 21:45-66.